

## Single-Crystal Nanowires of Platinum Can Be Synthesized by Controlling the Reaction Rate of a Polyol Process

Jingyi Chen,<sup>†</sup> Thurston Herricks,<sup>‡</sup> Matthias Geissler,<sup>†</sup> and Younan Xia<sup>\*,†</sup>

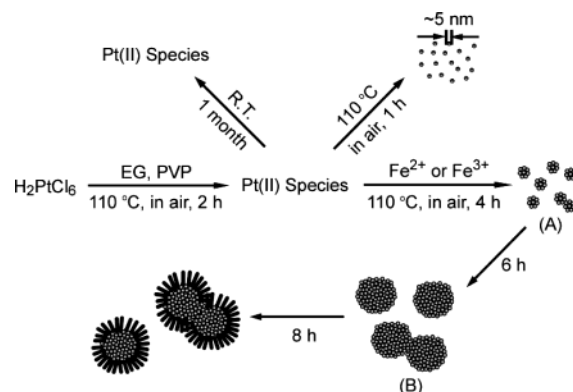
Department of Chemistry and Department of Materials Science and Engineering, University of Washington, Seattle, Washington 98195-1700

Received May 28, 2004; E-mail: xia@chem.washington.edu

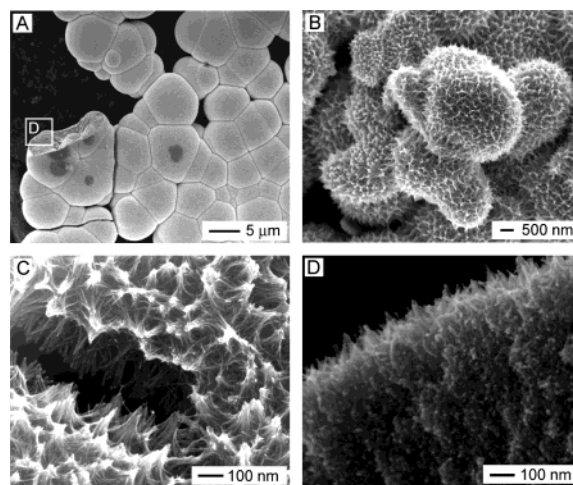
Platinum plays important roles in many applications because of its extraordinary physical and chemical properties.<sup>1</sup> For instance, it serves as a major catalyst in the industrial synthesis of nitric acid, reduction of pollutant gases emitted from automobiles, oil cracking, and proton-membrane-exchange (PME) fuel cells.<sup>2</sup> All these applications require the use of Pt in the finely divided state. For this reason, various chemical protocols have been developed for preparing Pt nanostructures.<sup>3</sup> Most of the work, however, has been limited to nanoparticles; only polycrystalline nanorods and nanotubes have been fabricated by templating against channels in porous materials<sup>4</sup> and Ag or Se nanowires.<sup>5</sup> Recently, Kijima et al. have also demonstrated the synthesis of Pt nanotubes by using surfactants as templates.<sup>6</sup> It remains a grand challenge to directly prepare Pt nanowires via a chemical route. Here we demonstrate, for the first time, that single-crystal nanowires of Pt could be synthesized in large quantities using the polyol process.<sup>7</sup> The key strategy is the introduction of a trace amount of Fe<sup>2+</sup> (or Fe<sup>3+</sup>) species to greatly reduce the level of supersaturation of Pt atoms and thus the growth rate by slowing down the reduction reaction. For the protocol described here, the Pt nanowires also assembled into hierarchical structures (like a sea urchin) during synthesis as a result of salt-induced agglomeration.

Figure 1 summarizes all major steps and changes involved in a typical synthesis. In this so-called polyol process, ethylene glycol (EG) serves as both a reducing agent and a solvent.<sup>8</sup> In the first step, Pt(II) species were formed when H<sub>2</sub>PtCl<sub>6</sub> or K<sub>2</sub>PtCl<sub>6</sub> was reduced by EG at 110 °C in the presence of poly(vinyl pyrrolidone) (PVP). At room temperature, the Pt(II) species were stable and no particles were formed when the solution was stored in a vial for one month. When the reaction continued in air at 110 °C, the Pt(II) species were reduced slowly to generate Pt nanoparticles with a diameter of ~5 nm (Figure S1A, Supporting Information). If a small amount of FeCl<sub>3</sub> or FeCl<sub>2</sub> was added (with a final concentration of 5 μM) after the reaction had proceeded for 2 h, Pt nanoparticles were produced at a relatively slower rate and tended to assemble into spherical agglomerates and larger structures. This agglomeration might be attributed to the destruction of the stabilization layer around each Pt nanoparticle. Interestingly, the Pt(II) species were reduced at an extremely slow rate by the end of the reaction, and the resultant Pt atoms started to nucleate and grow into uniform nanowires on the surface of each agglomerate. Note that PVP had to be present in the synthesis; otherwise, no Pt nanowires could be formed.

Figure 2 shows SEM images of a typical product at three different magnifications. Consistent with the drawing in Figure 1, the product contained micrometer-sized agglomerates of Pt nanoparticles, with the surface covered by a densely packed array of Pt nanowires. These agglomerates could be further fused into larger structures.



**Figure 1.** Schematic illustration detailing all major steps and changes involved in the formation of single-crystal Pt nanowires through an iron-mediated polyol process. The final product looks like sea urchins.



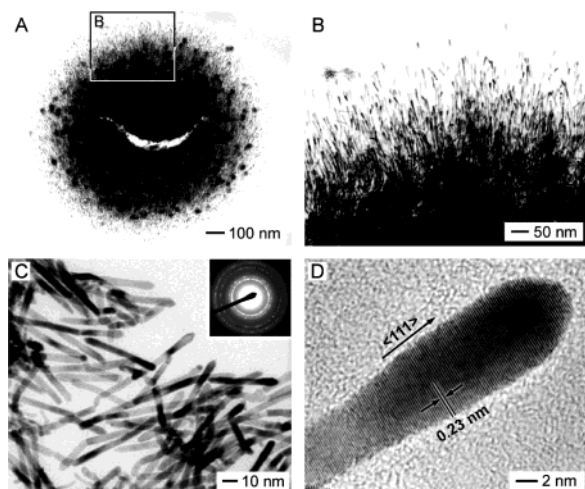
**Figure 2.** SEM images of hierarchically structured Pt agglomerates that were obtained as the final product of an iron-mediated polyol process: (A–C) overviews of the product at three different magnifications; (D) cross-sectional view of the edge of a particle as boxed in (A), showing that the interior of this particle was filled with Pt nanoparticles of ~5 nm in size, while the surface was covered by a thin layer of Pt nanowires.

Figure 2D shows an SEM image taken from the cross-sectional edge (as indicated by the box in Figure 2A) of an agglomerate, confirming that its interior, indeed, consisted of a densely packed lattice of Pt nanoparticles and that Pt nanowires could only be found on the surface of each agglomerate. EDX analysis also established that both the interior and the surface of the agglomerate were composed of elemental platinum.

To examine the hierarchical structure in more detail, we microtomed the agglomerate and then looked at its cross-section under TEM. A typical example is shown in Figure 3A. Figure 3B gives an enlarged image of the portion indicated by the box in Figure 3A. It is clear that the nanowires only covered the outer

<sup>†</sup> Department of Chemistry.

<sup>‡</sup> Department of Materials Science and Engineering.



**Figure 3.** (A) Cross-sectional TEM image of an individual agglomerate that was taken from its microtomed sample. (B) Enlarged TEM image of the edge of this particle, indicating that the Pt nanowires are uniaxially aligned in the plane of cleavage due to the shear force induced by the diamond knife. (C) TEM image and electron diffraction pattern of Pt nanowires that had been released from the surface of agglomerates via sonication. (D) HRTEM image of the tip of an individual Pt nanowire, indicating that it was a single crystal, with its growth direction along the  $\langle 111 \rangle$  axis.

surface of this agglomerate with a thickness of  $\sim 100$  nm, while the interior of this agglomerate contained a dense array of nanoparticles resembling the microscopic variant of a sea urchin with spines. Since the nanowires were loosely attached to the surfaces of agglomerates, it was possible to release them by brief sonication without breaking the agglomerates. Once freed, the nanowires could be recovered by centrifugation and then redispersed in ethanol or water without introducing additional surfactants. Figure 3C shows a typical TEM image of pure Pt nanowires ( $\sim 5$  nm in diameter) obtained using this procedure. The inset gives a selected-area electron diffraction (SAED) pattern, with the four rings indexed to the  $\{111\}$ ,  $\{200\}$ ,  $\{220\}$ , and  $\{311\}$  diffractions, respectively. We conclude that the Pt nanowires synthesized using this method are crystallized in a face-centered cubic (*fcc*) structure similar to the bulk solid. This claim is also supported by the XRD pattern (Figure S1D, Supporting Information), which was taken from a collection of nanowires of several syntheses. Figure 3D shows a HRTEM image recorded from the end of a single Pt nanowire, indicating that the nanowire grew along the  $\langle 111 \rangle$  direction. The lattice spacing between the  $\{111\}$  planes, 0.23 nm, is also in agreement with that of the bulk crystal.

In this synthesis, the presence of both iron species and air was critical to the formation of Pt nanowires. When the synthesis was performed under nitrogen gas, the reduction was much faster than in air, and only nanoparticles were formed. This observation implies that the absorption of oxygen from air on the surface of Pt nanoparticles was able to slow the autocatalytic reduction of Pt compounds.<sup>9</sup> On the basis of the results of XPS and UV–vis measurements, the overall reduction is believed to proceed in two steps, involving the formation of some Pt(II) intermediate species (Figure 1). Figure S2 shows the high-resolution XPS spectra in the Pt(4f) region, from which we could identify different oxidation states for Pt that were involved at different stages of the synthesis. The XPS data also served as a reference for assigning the peaks in the UV–vis spectra (Figure S3, Supporting Information) that were taken from the corresponding samples. The relevant data of UV–vis and XPS measurements are summarized in Table S1. These data suggest that Pt(IV) was fully reduced to Pt(II), and no Pt(0) was formed

after the reaction had proceeded for 2 h. Once the nucleation of Pt(0) particles had started, further reduction of the Pt(II) species was accelerated via an autocatalytic process. Although the presence of oxygen could slow this process, the reduction was still too fast to induce anisotropic growth. In contrast, reduction of the Pt(II) species was largely diminished when  $\text{Fe}^{2+}$  or  $\text{Fe}^{3+}$  was added to the reaction mixture, as depicted in Figure S3D. Since  $\text{Fe}^{2+}$  could be readily converted to  $\text{Fe}^{3+}$  by oxygen under the conditions used to perform the synthesis, the function of both  $\text{Fe}^{2+}$  and  $\text{Fe}^{3+}$  species seemed to be similar: to oxidize Pt(0) to Pt(II) (by  $\text{Fe}^{3+}$ ) and thus greatly reduce the supersaturation of Pt atoms. The resultant  $\text{Fe}^{2+}$  could be recycled to  $\text{Fe}^{3+}$  by oxygen, so that only a small amount of  $\text{Fe}^{2+}$  or  $\text{Fe}^{3+}$  was needed in this synthesis.

In summary, the polyol reduction could be significantly slowed to induce anisotropic growth in an isotropic medium by adding a small amount of  $\text{Fe}^{2+}$  or  $\text{Fe}^{3+}$  species. The initial product of such a synthesis was Pt nanoparticles ( $\sim 5$  nm in size) that existed in the form of micrometer-sized agglomerates. Once the supersaturation had been reduced to a certain level, the growth of Pt atoms would be switched to a highly anisotropic mode to form uniform Pt nanowires on the surface of each agglomerate. Since the Pt(II) species existed in the solution at a low concentration for a long period of time, the Pt atoms could grow into straight nanowires as long as  $\sim 100$  nm. After synthesis, the Pt nanowires could be separated from the agglomerates of Pt nanoparticles via a combination of brief sonication and centrifugation.

**Acknowledgment.** This work was supported in part by a DARPA-DURINT subcontract from Harvard University and a Fellowship from the David and Lucile Packard Foundation. Y.X. is a Camille Dreyfus Teacher Scholar. J.C. and T.H. thank the Center for Nanotechnology at the University of Washington for a Nanotech and an IGERT fellowship (funded by NSF, DGE-9987620), respectively. We are grateful to Deborah Leach-Scampavia for her help with XPS measurements.

**Supporting Information Available:** Experimental procedure; TEM and SEM images of various structures involved in the reaction; XRD pattern of the Pt nanowires; and high-resolution XPS spectra and UV–vis spectra taken at different stages of the reaction. This material is available free of charge via the Internet at <http://pubs.acs.org>.

## References

- (1) See, for example: Cotton, F. A.; Wilkinson, G. *Advanced Inorganic Chemistry*, 5th ed.; John Wiley & Sons: New York, 1988; p 868.
- (2) See, for example: (a) Rouxoux, A.; Schulz, J.; Patin, H. *Chem. Rev.* **2002**, *102*, 3757. (b) Williams, K. R.; Burstein, G. T. *Catal. Today* **1997**, *38*, 401.
- (3) See, for example: (a) Ahmadi, T. S.; Wang, Z. L.; Green, T. C.; Heglein, A.; El-Sayed, M. A. *Science* **1996**, *272*, 1924. (b) Teranishi, T.; Hosoe, M.; Tanaka, T.; Miyake, M. *J. Phys. Chem. B* **1999**, *103*, 3818. (c) Chen, S.; Kimra, K. *J. Phys. Chem. B* **2001**, *105*, 5397. (d) Wakayama, H.; Setoyama, N.; Fukushima, Y. *Adv. Mater.* **2003**, *15*, 742.
- (4) (a) Sakamoto, Y.; Fukuoka, A.; Higuchi, T.; Shimomura, N.; Inagaki, S.; Ichikawa, M. *J. Phys. Chem. B* **2004**, *108*, 853. (b) Husain, A.; Hone, J.; Postma, H. W. C.; Huang, X. M. H.; Drake, T.; Barbic, M. *Appl. Phys. Lett.* **2003**, *83*, 1240. (c) Fu, X.; Wang, Y.; Wu, N.; Gui, L.; Tang, Y. *J. Mater. Chem.* **2003**, *13*, 1192. (d) Arbiol, J.; Cabot, A.; Morante, J. R.; Chen, F.; Liu, M. *Appl. Phys. Lett.* **2002**, *81*, 3449. (e) Shin, H. J.; Ryoo, R.; Liu, Z.; Terasaki, O. *J. Am. Chem. Soc.* **2001**, *123*, 1246. (f) Han, Y.; Kim, J.; Stucky, G. D. *Chem. Mater.* **2000**, *12*, 2068. (g) Martin, C. R. *Science* **1994**, *266*, 1961. (h) Keating, C. D.; Natan, M. J. *Adv. Mater.* **2003**, *15*, 451. (i) Martin, B. R.; Dermody, C. J.; Reiss, B. D.; Fang, M.; Lyon, L. A.; Natan, M. J.; Mallouk, T. E. *Adv. Mater.* **1999**, *11*, 1021.
- (5) (a) Sun, Y.; Mayers, B.; Xia, Y. *Adv. Mater.* **2003**, *15*, 641. (b) Mayers, B.; Jiang, X.; Sunderland, D.; Cattle, B.; Xia, Y. *J. Am. Chem. Soc.* **2003**, *125*, 13364.
- (6) Kijima, T.; Yoshimura, T.; Uota, M.; Ikeda, T.; Fujikawa, D.; Mouri, S.; Uoyama, S. *Angew. Chem., Int. Ed.* **2004**, *43*, 228.
- (7) See Supporting Information for full experimental description.
- (8) Fievet, F.; Lagier, J. P.; Figlarz, M. *MRS Bulletin* **1989**, December, 29.
- (9) Mallat, T.; Baiker, A. *Catal. Today*, **1994**, *19*, 247.

JA0468224